JOURNAL OF AGRICULTURAL AND FOOD CHEMISTRY

Bioactive Constituents, Metabolites, and Functions

New Acylated Phenolic Glycosides with ROS Scavenging Activity from Psidium guajava Leaves

Yuanyuan Li, Dongli Li, Qi An, Hang Ma, Yu Mu, Wenjun Qiao, Zengguang Zhang, Jingsheng Zhang, Xueshi Huang, and Liya Li

J. Agric. Food Chem., **Just Accepted Manuscript** • DOI: 10.1021/acs.jafc.9b04318 • Publication Date (Web): 11 Sep 2019

Just Accepted

is published by the American Chemical Society. 1155 Sixteenth Street N.W., Washington, DC 20036

New Acylated Phenolic Glycosides with ROS Scavenging Activity from *Psidium guajava* Leaves

Yuanyuan Li, † Dongli Li, ‡ Qi An,† Hang Ma, ‡,§ Yu Mu,† Wenjun Qiao, ¶ Zengguang Zhang, † Jingsheng Zhang, ¶ Xueshi Huang, *,† and Liya Li*,†

† Institute of Microbial Pharmaceuticals, College of Life and Health Sciences, Northeastern University, Shenyang 110819, P. R. China

‡ School of Biotechnology and Health Sciences, Wuyi University, Jiangmen 529020, P. R. China

§ Bioactive Botanical Research Laboratory, Department of Biomedical and Pharmaceutical Sciences, College of Pharmacy, University of Rhode Island, Kingston, RI, 02881, United States

¶ Affiliated Hospital of Liaoning University of Traditional Chinese Medicine, Shenyang 110032, P. R. China

**Author to whom correspondence should be addressed*

Phone/Fax: 401-874-9367/5787; E-mail: huangxs@mail.neu.edu.cn

Phone/Fax: 0086-24-83656122; E-mail: lyli@mail.neu.edu.cn

ABSTRACT: ROS and subsequent oxidative stress are reported to play important roles in chronic metabolic diseases. Plant-derived polyphenols, especially food-derived phenolics, have attracted a lot of attention due to their potential usage against oxidative stress-related diseases. The leaf of *Psidium guajava* (known as guava) is regarded as a good resource of polyphenols and its products are commercially available in Japan as functional foods against multiple chronic metabolism disorders. In the course of finding novel polyphenols with antioxidative activities from guava leaf, eleven acylated phenolic glycosides (**1**-**11**), including five new oleuropeic acid conjugated phenolic glycosides, named guajanosides A-E (**1**, **2**, and **5**-**7**), along with 17 known meroterpenoides (**12**-**28**) were isolated and identified. Their structures were determined by spectroscopic data analysis, chemical degradation and acid hydrolysis. Compounds **1, 2,** and **5-11** displayed potent reactive oxygen species (ROS) scavenging activity in LPS-stimulated RAW 264.7 macrophage cells. Western blot revealed that compound **6** markedly increased the expression levels of nuclear factor-erythroid 2-related factor 2 (Nrf2), NAD(P)H quinone dehydrogenase 1 (NQO1) and glutamate-cysteine ligase catalytic subunit (GCLC). The current study revealed the presence of oleuropeic acid-derived phenolic glycosides in guava leaf, and highlighted the potential usage of this type of phenolics against oxidative stress-related metabolic diseases via activation of Nrf2 signaling pathway.

KEYWORDS: *Psidium guajava, guava leaf, acylated phenolic glycosides, ROS scavenging activity, Nrf2 signaling pathway*

INTRODUCTION

Reactive oxygen species (ROS) are a group of oxygen-containing redox-active intermediates released by endogenous and exogenous processes.[1] Although ROS have been reported to play important roles in signaling cascade for normal physiological functions, elevated cellular ROS levels which overcome endogenous antioxidant capacity would cause oxidative stress condition and damage multiple biomolecules.[2, 3] ROS and subsequent oxidative stress are reported to be implicated in multiple chronic metabolic diseases, such as diabetes, cardiovascular disease, and neurodegenerative disease.[1, 4] Thus, maintaining redox homeostasis is essential for normal physiological process in human body. Emerging evidences have demonstrated that natural antioxidants could play positive effects against oxidative stress-induced chronic metabolic diseases by acting as ROS scavengers.[5, 6] Nuclear factor erythroid 2-related factor 2 (Nrf2), which is expressed in a wide range of tissues and cell types, is a crucial transcription factor involved in oxidation defensive system.[7] Although Nrf2 in the cytoplasm undergoes rapidly proteasomal degradation in the physiological condition, it will be accumulated and translocated into nucleus under oxidative stress condition, leading to the up-regulation of many antioxidant related enzymes, such as quinine oxidoreductase 1 (NQO1) and γ-glutamyl cysteine synthetase catalytic subunit (GCLC) to restore cellular redox homeostasis.[8, 9] Extensive evidences demonstrate that Nrf2 signaling pathway plays a pivotal role in the prevention of cell injury resulting from oxidative stress.[10] A lot of polyphenols, especially food-derived polyphenols, have been found to active Nrf2 signaling pathway to reduce ROS production, and then exert health

beneficial effects.[9]

Psidium guajava L., also known as guava, belongs to the family of Myrtaceae. Being important food crop, guava is cultivated in the tropical and subtropical regions worldwide, including south of China.[11, 12] Besides the popular usage of its edible fruit in food industry, guava leaf is also widely consumed as beverage in Japan, China and Korea against multiple chronic diseases, such as diabetes and obesity.[13, 14] Guava Leaf Tea (Bansoureicha®, Yakult Honsha, Tokyo, Japan) has been approved and commercially available as one of the Foods for Specified Health Uses in Japan,[11] and regarded as a potential natural source for finding novel bioactive compounds against metabolic diseases.[10, 13] Previous phytochemical studies have revealed that abundant polyphenols, including flavonoids,[15] tannins,[16] meroterpenoides[17] and benzophenones[11] are present in guava leaves. During the process of finding bioactive chemical constituents against chronic metabolic diseases from guava leaves, five new oleuropeic acid conjugated phenolic glycosides (**1**, **2**, and **5-7**) and six known analogues (**3**, **4**, and **8-11**), as well as 17 known meroterpenoides (**12**−**28**) were isolated and identified from guava leaves. Oleuropeic acid conjugated phenolic glycosides are a group of phenolics mainly found from Myrtaceous plants, especially from the genus *Eucalyptus*.[18, 19, 20] The numbers of this type of phenolics reported are very limited (less than 40). They usually possess a 5,7-dihydroxychromone, flavonone, or gallic acid skeleton, and are conjugated with oleuropeic acid fragment. Previous pharmacological studies revealed that this type of compounds possessed anti-tumor,[21] anti-inflammatory,[22] anti-melanogenesis,[22] and antibacterial activities.[23] To the best of our knowledge, this is the

first report of oleuropeic acid conjugated phenolic glycosides from guava. Meanwhile, to date, there is scarce of data about the ROS scavenging effect and mechanism of action of this type of compounds.

Thus, we initiate the current study with following objectives: (1) to investigate the underlying mechanisms of antioxidant action of these new acylated phenolic glycosides, as well as (2) to better understand the relationship between the present acylated phenolic glycosides and the health beneficial effects attributed to guava leaf. Macrophages are crucial for the immune system and are vulnerable to ROS. Bacterial lipopolysaccharide (LPS), an important component of the cell walls of gram-negative bacteria, can promote the production of ROS in macrophages and impact Nrf2 signaling pathway.[24] LPS-stimulated RAW 264.7 macrophage is widely accepted as a suitable model for the ROS-scavenging activity evaluation and related mechanism study.[7, 24, 25]

Herein, we reported the isolation and structure elucidation of acylated phenolic glycosides from guava leaves. In addition, ROS scavenging activities of these isolates were evaluated with LPS-stimulated RAW 264.7 cells. We also attempted to elucidate the underlying mechanisms of antioxidant action of these acylated phenolic glycosides by investigating the involvement of the Nrf2 signaling pathway.

MATERIALS AND METHODS

General Experimental Procedures. Optical rotations were determined in MeOH or $CHCl_3$ using an Anton Paar MCP200 automatic polarimeter (Graz, Austria). IR spectra were measured with a Bruker Tensor 27 FT–IR spectrometer (film). Ultraviolet spectra were recorder with a Beckman Coulter DU 730 nucleic acid/protein analyzer

(Brea, CA, USA). One- and two-dimensional NMR spectra were collected on a Bruker Advance III-600 MHz spectrometer (Bruker Co., Rheinstetten, Germany) with dimethyl sulfoxide (DMSO-d_6) as the solvent. Semi-preparative HPLC was performed using an ODS column (250 mm × 10 mm, 5 μm, YMC-ODS-A, YMC Co. Ltd., Kyoto, Japan). ESI-MS were recorded on an Agilent 1290-6420 Triple Quadrupole LC-MS spectrometer (Santa Clara, CA, USA). HRESIMS was measured either with a Bruker Micro TOF-Q mass spectrometer (Bruker Daltonics, Billerica, MA) or a Shimadzu MALDI-TOF mass spectrometer (Shimadzu Corporation, Kyoto, Japan). Absorbance and fluorescence values were analyzed using a microplate reader (BioTek Synergy H1, BioTek Instruments, Winooski, VT, USA). Silica gel (100-200 mesh, 300-400 mesh, Qingdao Marine Chemical Ltd., Qingdao, China), Sephadex LH-20 (GE Healthcare Biosciences AB, Uppsala, Sweden), MCI gel (CHP-20P, Mitsubishi Chemical Corp., Tokyo, Japan), and ODS-A (S-50 μm, 12 nm, YMC Co., Ltd., Kyoto, Japan) were used for column chromatography. D-glucose, L-glucose, D-galactose, and L-galactose were got from Sinopharm Chemical Reagent Co., Ltd. (Shenyang, People's Republic of China). L-cysteine methyl ester hydrochloride was purchased from Maya Reagent (Jiaxing, China). LPS, 3-[4,5-Dimethylthiazol-2-yl]-2,5-diphenyltetrazolium bromide (MTT), and minocycline (MINO) were obtained from Sigma Chemical Co. (St. Louis, MO, USA). All other chemicals and solvents were purchased from Sinopharm Chemical Reagent Co., Ltd.

Plant Material. The leaves of *P. guajava* were collected from Guangdong Province, in August 2016. The plant was identified by Professor Xiaoji Zheng

(Guangdong Jiangmen Chinese Traditional Medicine College, Jiangmen, China). A voucher specimen (NO 1610056) was deposited at the Institute of Microbial Pharmaceuticals, Northeastern University.

Extraction and Isolation. The air-dried leaves (4.0 kg) of *P. guajava* were powdered and defatted with petroleum ether (2 × 10 L) at room temperature. The residue was then extracted with 75% ethanol (3 × 20 L, 3 days each) at room temperature for three times. The supernatant was combined and evaporated under reduced pressure to afford a crude ethanol extract (1.0 kg). The ethanol extract was then suspended in water and partitioned successively with petroleum ether (3 × 20 L), ethyl acetate (3 × 20 L), and *n*-BuOH (3 × 20 L). After solvent removal, the ethyl acetate extract (200.0 g) was subjected to a MCI gel CHP-20P column, eluting with MeOH-H_2O system (0, 20, 40, 60, 80, and 100%) to afford six fractions A-F. Fraction D (30.0 g, 60% MeOH eluted fraction) was subjected to silica gel column chromatography (CH_2Cl_2/MeOH 50:1, v/v) to yield three subfractions (D1-3). Subfraction D1 was separated by ODS column (MeOH/H_2O 60%, v/v) and purified by Sephadex LH-20 column chromatography with MeOH to yield compound **1** (5.9 mg). Subfraction D2 was chromatographed over an ODS column with (MeOH/H_2O 60%, v/v) elution system to yield compounds **2** (10.0 mg) and **10** (15.0 mg). Subfraction D3 was successively subjected to silica gel (CH_2Cl_2/MeOH 30:1, v/v), ODS (MeOH/H_2O 60%, v/v) and Sephadex LH-20 column (MeOH) to yield compounds **3** (59.2 mg) and **11** (20.6 mg). Fraction E (35.0 g, 80% MeOH eluted fraction) was put on a Sephadex LH-20 column and eluted with MeOH to yield three subfractions (E1-3). Subfraction E1 was

132 successively chromatographed over silica gel column (CH_2Cl_2/MeOH 30:1, v/v), ODS
133 column (MeOH/H_2O 60%, v/v), and semi-preparative HPLC (55% MeOH/H_2O, v/v) to
134 yield compounds **4** (20.0 mg), **6** (6.8 mg), and **7** (7.5 mg). Subfraction E2 was separated
135 over ODS column (MeOH/H_2O 65%, v/v) to afford compound **8** (100.0 mg).
136 Subfraction E3 was chromatographed over a silica gel column (CH_2Cl_2/MeOH, 20:1,
137 v/v), and further purified by semi-preparative HPLC (45% MeOH/H_2O, v/v) to yield
138 compound **9** (13.6 mg). In addition, the petroleum ether extract (160.0 g) of guava
139 leaves was chromatographed over silica gel, ODS, Sephadex LH-20, and semi-
140 preparative reversed-phase HPLC to afford 17 known meroterpenoides (**12**-**28**).
141 Detailed isolation procedures for these known compounds are provided in the
142 Supporting Information.

143 *Compound* **1**: yellow amorphous powder; $[\alpha]_D^{20}$ +8.0 (c 1.0, MeOH); UV (MeOH)
144 λ_{max} (log ε) 296 (3.54), 258 (4.03), 214 (4.31) nm; IR (film) ν_{max} 3346 , 2960, 2879,
145 1702, 1661, 1620, 1591, 1424, 1390, 1357, 1259, 1178, 1079, 1025, 917 cm^{-1}; ^1H and
146 ^{13}C NMR data (in DMSO-d_6) see Table 1; HRESI-MS *m/z* 1039.3823 $[2M-H]^-$ (calcd
147 for $C_{52}H_{63}O_{22}$, *m/z* 1039.3811).

148 *Compound* **2**: yellow amorphous powder; $[\alpha]_D^{20}$ -27.5 (c 1.8, MeOH); UV (MeOH)
149 λ_{max} (log ε) 296 (3.89), 258 (4.46), 214 (4.81) nm; IR (film) ν_{max} 3357 , 2961, 2929,
150 2873, 1710, 1658, 1621, 1588, 1429, 1369, 1273, 1248, 1079, 1025, 1003, 916 cm^{-1};
151 ^1H and ^{13}C NMR data (in DMSO-d_6) see Table 1; HRESI-MS *m/z* 1123.4754 $[2M-H]^-$
152 (calcd for $C_{58}H_{75}O_{22}$, *m/z* 1123.4750).

153 *Compound* **5**: white amorphous powder; $[\alpha]_D^{20}$ -20.0 (c 1.0, MeOH); UV (MeOH)

λ_{max} (log ε) 258 (4.13), 218 (4.78), 196 (4.75) nm; IR (film) ν_{max} 3371, 2967, 2931, 1699, 1649, 1596, 1435, 1389, 1351, 1256, 1220, 1147, 1109, 924 cm^{-1}; ^{1}H and ^{13}C NMR data (in DMSO-d_6) see Table 1; HRESI-MS *m/z* 511.1812 $[M-H]^-$ (calcd for $C_{24}H_{31}O_{12}$, *m/z* 511.1816).

Compound **6**: yellow amorphous powder; $[\alpha]_D^{20}$ -12.0 (c 1.0, MeOH); UV (MeOH) λ_{max} (log ε) 354 (4.53), 258 (3.77), 192 (4.61) nm; IR (film) ν_{max} 3274, 2924, 2855, 1701, 1652, 1604, 1496, 1443, 1358, 1300, 1269, 1201, 1170, 1069, 1022, 997, 935 cm^{-1}; ^{1}H and ^{13}C NMR data (in DMSO-d_6) see Table 2; HRESI-MS *m/z* 1223.3628 $[2M-H]^-$ (calcd for $C_{62}H_{63}O_{26}$, *m/z* 1223.3608).

Compound **7**: yellow amorphous powder; $[\alpha]_D^{20}$ +20.0 (c 0.6, MeOH); UV (MeOH) λ_{max} (log ε) 354 (3.96), 258 (4.17), 192 (4.73) nm; IR (film) ν_{max} 3339, 2923, 2854, 1698, 1651, 1604, 1507, 1445, 1359 1303, 1263, 1201, 1169, 1088, 1024, 999, 935 cm^{-1}; ^{1}H and ^{13}C NMR data (in DMSO-d_6) see Table 2; HRESI-MS *m/z* 1223.3604 $[2M-H]^-$ (calcd for $C_{62}H_{63}O_{26}$, *m/z* 1223.3608).

Acid Hydrolysis and Monosaccharide Determination of Compounds 5-7. Acid hydrolysis of compounds **5-7** were performed according to a previously reported method.[26] Briefly, compounds **5-7** (each 2 mg) were dissolved in 0.5 mL of MeOH and then hydrolyzed with 2 M HCl (2 mL) at 80 °C for 4 h. After cooling, the yield mixture was washed with CH_2Cl_2 (2 mL) for three times, and the aqueous layer was dried with evaporator *in vacuo*. The dried powder was then dissolved in pyridine (1 mL) and reacted with L-cysteine methyl ester hydrochloride (2 mg) at 80 °C with stirring for 2 h. Then *N*-trimethylsilylimidazole (0.3 mL) was added and reacted at 80 °C for another

2 h. After that, 1 M HCl (5 mL) was added to the mixture and then extracted with hexane (5 mL) for three times. The hexane extract was combined and submitted for GC-MS analysis. Gas chromatography was performed with a Shimadzu GCMS-QP2020 gas chromatograph mass spectrometer (Shimadzu Corporation, Kyoto, Japan) equipped with an AOC-20i auto injector (Shimadzu Corporation). The separation was conducted over a SH-Rxi-5Sil MS capillary column (30 m × 0.25 mm × 0.25 μm, Shimadzu Corporation) at a flow rate of 1 mL/min with a split ratio of 12:1. Helium was used as carrier gas and the injection volume was 1 μL. The inlet temperature was set as 270 °C. The initial oven temperature was 180 °C and raised to 280 °C by 5 °C/min, hold for 3 min, and then reached 300 °C by 20 °C/min, and hold for 4 min. The retention time of derivatives of standard D-glucose, L-glucose, D-galactose, and L-galactose were 13.45, 13.74, 13.84 and 14.21 min, respectively. The configurations of D-glucose for compounds **5** and **6,** and D-galactose for compound **7** were determined based on comparison of the retention time of corresponding derivatives with those of authentic sugars derivatives prepared in the same method.

Methanolysis of Compound 8. A solution of compound **8** (6.7 mg) in MeOH (1 mL) containing 1% NaOMe was stirred at room temperature for 12 h. Then two drops of AcOH was added and the yield mixture was dried under vacuum. The residue was subjected to preparative thin layer chromatography (CH_2Cl_2/MeOH 15:1, v/v) to yield (+)-oleuropeic acid methyl ester **1b** (2.6 mg): $[\alpha]_D^{20}$ +76.0 (c 1.0, $CHCl_3$). ^{1}H-NMR (in $CDCl_3$, 600 MHz): δ_H 7.01 (m, 1H, H-2), 3.75 (s, 3H, -OCH_3), 2.56 (m, 1H, H-6a), 2.36 (m, 1H, H-3a), 2.20 (m, 1H, H-6b), 2.04 (m, 1H, H-3b), 2.01 (m, 1H, H-5a), 1.57 (m,

198 1H, H-5b), 1.57 (m, 1H, H-4), 1.24 (s, 3H, H-10), 1.23 (s, 3H, H-9). ^{13}C-NMR (in
199 $CDCl_3$, 150 MHz): δ_C 130.1 (C-1), 139.4 (C-2), 27.3 (C-3), 44.1 (C-4), 23.3 (C-5), 25.2
200 (C-6), 167.8 (C-7), 72.4 (C-8), 26.6 (C-9), 27.4 (C-10), 51.6 (-OCH_3).

201 **DPPH Assay.** The DPPH free radical scavenging assay was performed according
202 to previously reported method.[25] Briefly, a series of different concentrations of the
203 tested samples and the positive control ascorbic acid (6.25 to 200 μM) were mixed with
204 freshly prepared DPPH (0.2 mM) in a 96-well microplate with total volume of 150 μL.
205 After leaving the mixture reacted in the dark for 30 min, its absorbance was determined
206 at 520 nm. All the wells with sample only were set as blank to obtain an absorbance
207 value which was subtracted from the test sample readings. The free radical scavenging
208 capacity was calculated using the following equation: $\%\ SC = \frac{A_{control} - (A_{sample} - A_{blank\ sample})}{A_{control}}$
209 $\times 100\%$. The IC_{50} values were calculated by SPSS 17.0 statistic software. Results were
210 expressed as the mean ± SD of three replicates.

211 **Reactive Oxygen Species Scavenging Assay.** ROS scavenging activity of
212 compounds **1-11** were evaluated with LPS-induced RAW 264.7 cell model.
213 Intracellular ROS were determined by using a fluorescent probe 2′,7′-dichlorofluoresin
214 diacetate (DCFH-DA) (Beyotime Biotechnology, Shanghai, China), according to the
215 manufacturer's instructions. Briefly, RAW 264.7 cells cultured in DMEM medium
216 were seeded in 96-well-plates with 3×10^4 cells/well. After incubation for 24 h, LPS (1
217 μg/mL) and the tested samples (final concentrations at 30 μM) were added and co-
218 incubated for another 6 h. Then the supernatant of each well was removed and serum-
219 free medium with DCFH-DA (10 μM) were added into wells for 60 min treatment in

the dark. After that, cells were washed with phosphate buffered saline and the fluorescence of each well was measured by using a microplate reader at an emission wavelength of 525 nm and an excitation wavelength of 488 nm. Minocycline (MINO) was used as the positive control. All samples were tested in triplicate and showed no cell toxicity against RAW 264.7 cells at 30 μM as shown in MTT assay (See Supporting Information Figure S51).

Western Blotting. Compound **6** was selected for antioxidative mechanism study due to its superior activity in ROS scavenging assay. The effects of compound **6** on Nrf2 as well as its target downstream genes GCLC and NQO1 were investigated by western blot experiment. RAW 264.7 cells were seeded at a 1×10^6 cells per well in a 6-well plate. After 24 h incubation, the cells were pretreated with different concentrations of compound **6** (3.3, 10 or 30 μM) for 2 h, followed by exposure to LPS (1 μg/mL) for additional 6 h. After that, cells were lysed with a RIPA buffer and then centrifuged at 15 000 g for 15 min at 4 °C. The protein lysates were resolved by 10% sodium dodecyl sulfate polyacrylamide gel electrophoresis (SDS-PAGE), and electrophoretically transferred to PVDF membrane. The membrane was then blocked with 5% (w/v) non-fat dry milk in TBST, and then incubated with specific primary antibodies to Nrf2, GCLC, and NQO1 (Cell Signaling Technology, Danvers, MA, USA) at 4 °C overnight. B-actin was used as a loading control. Next day, the membrane was incubated with goat anti-rabbit IgG-HRP secondary antibody (Cell Signaling Technology, Danvers, MA, USA) at room temperature for 1 h. Chemiluminescence using ECL detection kit (GE Healthcare, Piscataway, NJ, USA) was detected by using

Bio-Rad ChemiDoc™ XRS+ System (Bio-Rad, Hercules, CA, USA). The experiment was repeated for three times.

Statistical Analysis. Quantitative data was presented as mean ± S.E. The statistical analysis was performed by GraphPad Prism 4.0 (GraphPad Software Inc., USA) and SPSS 17.0 (IBM., USA). The statistical significance between groups was interpreted by one-way ANOVA followed by Tukey's test. All statistical tests with $p < 0.05$ were considered significantly different.

RESULTS AND DISCUSSION

The ethyl acetate extract of *P. guajava* leaves was subject to column chromatography over MCI gel, silica gel, Sephadex LH-20 and semi-preparative HPLC to yield 28 phenolics, including 11 acylated phenolics glycosides (**1-11**) and 17 meroterpenoides (**12-28**). Their structures were determined on the basis of spectroscopic data analysis, chemical degradation, acid hydrolysis, as well as by comparison of these to literature data (Figure 1). Among these isolates, five oleuropeic acid conjugated phenolic glycosides (**1, 2,** and **5-7**) are new compounds, and another 14 compounds (**3**, **4**, **8-10**, and **12-20**) are reported from this plant for the first time.

Structure Elucidation of Isolated Phenolics. Compound **1** was obtained as yellow amorphous powder, $[\alpha]_D^{20}$ +8.0 (c 1.0, MeOH). The negative HR-ESIMS of **1** gave a quasimolecular peak at *m/z* 1039.3823 $[2M-H]^-$, corresponding to the molecular formula of $C_{26}H_{32}O_{11}$ with 11 indices of hydrogen deficiency. The IR spectrum of **1** showed absorption bands of hydroxyl (3346 cm^{-1}), carbonyl (1702 and 1661 cm^{-1}), and aromatic ring (1620 and 1591 cm^{-1}) functionalities. The UV spectrum of **1** showed

absorption maximum at 292 and 256 nm, indicating its 5,7-dihydroxychromone skeleton.[27] This conclusion was supported by ^{1}H NMR data of **1** (in DMSO-d_6, 600 MHz, Table 1) which showed the presence of a hydroxyl group (δ_H 13.00, s, 1H, OH-5), two singlet aromatic protons (δ_H 6.14, s, 1H, H-3; δ_H 6.18, s, 1H, H-6), and a singlet methyl group at δ_H 2.31 (s, 3H, 2-Me). ^{1}H NMR spectrum of **1** also revealed the presence of an olefinic proton (δ_H 6.90, m, H-2″), two singlet methyl groups (δ_H 1.05, s, 6H, H_3-9″ and H_3-10″), and an anomeric proton of a glycosyl group (δ_H 4.64, d, 1H, J = 10.2 Hz, H-1′). The ^{13}C NMR and DEPT spectra of **1** displayed 26 resonances ascribed to two carbonyl carbons, two olefinic carbons, eight aromatic carbons, one oxygenated tertiary carbon, six methines (five oxygenated), four methylenes (one oxygenated), and three methyls. All of the proton signals were assigned to the corresponding carbons by HSQC spectrum analysis. The NMR data of **1** resembled those of the known compound 8-*β*-*C*-glucopyranosyl-5,7-dihydroxy-2-methylchromone (isobiflorin), which was isolated from Myrtaceae family previously,[27] indicating compound **1** also possessed a 5,7-dihydroxy-2-methylchromone skeleton and *C*-glucosyl residue. The linkage of the glucosyl moiety to chromone skeleton through C-8 was deduced based on HMBC correlation signals from anomeric proton of glucose (H-1′) to C-7 (δ_C 165.1), C-8 (δ_C 104.6) and C-9 (δ_C 157.1). The *β*-configuration of glucose was determined by the large J value of H-1′ (10.2 Hz).[28] Further comparison of NMR data of **1** with isobiflorin revealed additional signals of a monoterpene, which was deduced as oleuropeic acid based on COSY and HMBC experiments. The linkage of oleuropeic acid moiety to *β*-glucose at C-6′ was established by the HMBC

correlations from H-6′a (δ_H 4.30, m, 1H) to carbonyl carbon at δ_C 166.8 (C-7″), and supported by the remarkable downfield shift of C-6′ (ca. 3 ppm), as well as upfield shift of C-5′ (ca. 3 ppm) when compared to isobiflorin.[27] Although determination of the absolute stereochemistry of oleuropeic acid unit in **1** with chemical degradation was difficult due to its limited quantity, the presence of I-oleuropeoyl was deduced based on the co-isolation of (+)-I-oleuropeic acid (**1a**) ($[\alpha]_D^{20}$+76.0, $CHCl_3$) from guava leaves in the current project. This assumption was further supported by the methanolysis of compound **8**, another oleuropeic acid derivative isolated in the current project, which gave (+)-I-oleuropeic acid methyl ester (**1b**) ($[\alpha]_D^{20}$+76.0, $CHCl_3$).[19] On the basis of above evidence, the structure of compound **1** was determined as 8-*β*-*C*-(6′-*O*-oleuropeoyl)-glucopyranosyl-5,7-dihydroxy-2-methylchromone and named as guajanoside A.

Compound **2** was obtained as yellow amorphous powder, $[\alpha]_D^{20}$ -27.5, (c 1.8, MeOH). The molecular formula of **2** was deduced as $C_{29}H_{38}O_{11}$ based on the quasimolecular peak at *m/z* 1123.4754 $[2M-H]^-$ in negative HRESIMS and ^{13}C NMR data. The IR spectrum of **2** highly resembled to that of **1**. Comparison of the 1D NMR data with those of compound **1** suggested the structure of compound **2** was also composed of oleuropeoyl and 8-*β*-*C*-glucopyranosyl-5,7-dihydroxychromone moieties. However, a group of proton signals for isobutyl group (δ_H 2.52, d, 2H, J = 7.2 Hz, H_2-1‴; δ_H 2.26, m, 1H, H-2‴; δ_H 1.00, d, 6H, J = 6.6 Hz, H_3-3‴ and H_3-4‴), which was deduced based on the ^1H-^1H COSY experiment (as shown in Figure 2), rather than methyl group were observed in **2**, indicating the substitute at C-2 in **2** was replaced by

isobutyl group. This conclusion was confirmed by the HMBC correlations from H-1‴ to C-2 (δ_C 170.0), C-3 (δ_C 108.5), C-2‴ (δ_C 26.9), C-3‴ (δ_C 22.7) and C-4‴ (δ_C 22.7), and supported by HRESIMS data. In addition, HMBC correlation signal from glucosyl H-2′ (δ_H 5.42, t, 1H, J = 10.2 Hz) to oleuropeoyl carboxylic carbon at δ_C 166.1 suggested the C-2′ linkage of oleuropeoyl group. This conclusion was supported by observed upfield chemical shifts of C-1′, C-3′, C-6′, as well as downfield chemical shifts of C-2′ and C-5′ in the glucosyl moiety relative to **1** due to esterification effect (Table 1). The absolute stereochemistry of oleuropeoyl group in **2** was also assigned as I like **1** as discussed above. Consequently, the structure of compound **2** was determined as 8-*β*-*C*-(2′-*O*-oleuropeoyl)-glucopyranosyl-5,7-dihydroxy-2-isobutylchromone and named as guajanoside B.

Compound **5** was obtained as a white amorphous powder. Its molecular formula, $C_{24}H_{32}O_{12}$, was established on the negative HR-ESIMS (*m/z* 511.1812 $[M-H]^-$, calcd 511.1816) and ^{13}C NMR data. The IR spectrum of **5** suggested the presence of hydroxyl group (3371 cm^{-1}), carbonyl (1699 and 1649 cm^{-1}), and benzene ring (1597 cm^{-1}) functionalities. Analysis of the ^1H and ^{13}C NMR spectra of **5** revealed it also had *β*-glucopyranosyl and oleuropeoyl groups. In addition, ^1H NMR spectrum of **5** showed the presence of two singlet aromatic protons (δ_H 7.04, H-2; δ_H 7.08, H-6) and a methoxyl group (δ_H 3.72, s, 3H). The ^{13}C NMR spectrum of **5** showed six characteristic aromatic carbon signals at δ_C 105.3, 111.1, 136.9 × 2, 150.4, and 152.9. The 1D NMR data of **5** resembled to known compound eucalmaidin B,[19] which was an oleuropeic acid derivative possessed a gallic acid unit in the structure. By comparison of 1D NMR

data of **5** with those of eucalmaidin B, an extra methoxyl group (δ_H 3.72, s; δ_C 56.5) was observed, which suggested one of the 17ethane17 groups on gallic acid fragment in eucalmaidin B was methylated. In the HMBC spectrum, the correlation signals from methoxyl protons to C-3 (δ_C 152.9) indicated methoxyl group was connected to C-3 of gallic acid. Additionally, the *β*-glucopyranose moiety located at C-4 was determined based on weak but detectable HMBC correlation between the aromatic proton (δ_H 4.78, d, 1H, J = 7.2 Hz, H-1′) and C-4 (δ_C 136.9). Acid hydrolysis of **5** with 2 M HCl liberated D-glucose, which was determined by subsequent GC-MS analysis following derivatization to trimethylsilylated L-cysteine adduct. The presence of *R*-oleuropeoyl unit was determined based on the co-isolation of **1a** and methanolysis result of known compound **8**. Therefore, the structure of **5** was determined as 4-*β*-*O*-(6′-*O*-oleuropeoyl)-glucopyranosyl-5-hydroxy-3-methoxybenzoate and named as guajanoside C.

Guajanoside D (**6**) was obtained as a yellow amorphous powder with $[\alpha]_D^{20}$ -12.0 (c 1.0, MeOH). Its molecular formula $C_{31}H_{32}O_{13}$ was elucidated from the HRESIMS (*m/z* 1223.3628 $[2M-H]^-$) and ^{13}C NMR data (Table 2). The IR spectrum of **6** showed absorption bands of hydroxyl (3274 cm^{-1}), carbonyl (1701 and 1652 cm^{-1}), and aromatic ring (1604 and 1496 cm^{-1}) functionalities. The ^1H NMR spectrum of **6** showed the presence of a hydroxyl group at δ_H 12.65 (5-OH), an ABX system at δ_H 6.82 (d, 1H, J = 8.4 Hz, H-5′), 7.50 (s, 1H, H-2′), and 7.52 (d, 1H, J = 8.4 Hz, H-6′), as well as two singlet aromatic protons at δ_H 6.17 (s, 1H, H-6) and 6.38 (s, 1H, H-8), suggesting the presence of a quercetin moiety. This conclusion was supported by UV and ^{13}C NMR

351 spectral data. In addition, 1D NMR data (Table 2) revealed the presence of β-glucosyl
352 with anomeric proton at δ_H 5.53 (d, 1H, J = 7.2 Hz, H-1″) and anomeric carbon at δ_C
353 100.7 (C-1″). Acid hydrolysis of **6** liberated D-glucose residue. Apart from these two
354 moieties, the ^{13}C NMR and DEPT data of **6** showed another 10 carbon signals,
355 including one carbonyl carbon (δ_C 166.3), four olefinic carbons (δ_C 149.0, 139.3, 129.6,
356 109.7), one 18ethane (δ_C 39.5), two methylenes (δ_C 30.7, 26.8, 24.4), and one methyl
357 (δ_C 21.1). The 1D NMR data of **6** highly resembled to those of known compound
358 **8**,[29].except that the signals for isopropanol unit in **8** were replaced by isopropenyl group
359 in **6**. This indicated that the oleuropeic acid unit in **8** was changed to perillic acid and
360 compound **6** was the dehydration derivative of **8**. This conclusion was confirmed by
361 HMBC correlation signals from H_2-9‴ (δ_H 4.67, s, 1H; 4.72, s, 1H) to C-4‴ (δ_C 39.5)
362 and C-10‴ (δ_C 21.1), and from H_3-10‴ (δ_H 1.69, s, 3H) to C-4‴ and C-9‴ (δ_C 109.7).
363 The absolute stereochemistry of C-4‴ in **6** was also assigned as I based on biogenesis
364 consideration. Thus, the structure of guajanoside D (**6**) was established as shown in
365 Figure 1.

366 Compound **7**, a yellow amorphous powder, had the same molecular formula of **6**
367 as $C_{31}H_{32}O_{13}$ deduced from its HRESIMS data (*m/z* 1223.3604 $[2M-H]^-$, calcd
368 1223.3608). The IR spectrum of **7** closely resembled to those of **6**. Analysis of 1D and
369 2D NMR data suggested high similarities between the structures of **6** and **7** except for
370 the sugar moiety. The monosaccharide in **7** was identified as β-D-galactopyranose by
371 comparison of its NMR data with literature,[30] along with acid hydrolysis and
372 subsequent GC-MS analysis. The HMBC correlations from H_2-6″ (δ_H 4.05, m, 2H) to

C-7‴ (δ_C 166.4) inferred that the monoterpene also located at C-6″ of *β*-D-galactose. The absolute stereochemistry of C-4‴ in **7** was also assigned as I like **6** based on biogenesis consideration. Thus, the structure of guajanoside E (**7**) was determined as depicted in Figure 1.

Besides guajanosides A-E, six known acylated phenolic glycosides, including cypellocarpin C (**3**),[31] eucamalduside A (**4**),[31] cypellogin A (**8**),[29] cypellogin B (**9**),[29] quercetin-3-*O*-*β*-D-(6''-*O*-*p*-coumaroyl)-galactopyranoside (**10**),[30] and guavaric A (**11**)[32] were also isolated and identified from guava leaves. Compounds **1**-**4** were glycosides bearing 5,7-dihydroxychromone, **5** was glycoside bearing galloyl group, whereas **6-11** were quercetin glycosides. All of the above phenol glycosides were esterified with (+)-oleuropeic acid except compounds **10** and **11**. In addition, 17 meroterpenoides, including euglobal B1-1 (**12**),[33] euglobal Ib (**13**),[33] euglobal Ic (**14**),[33] euglobal III (**15**),[34] euglobal Iib (**16**),[34] euglobal-Iva (**17**),[35] euglobal Ivb (**18**),[35] euglobal V (**19**),[36] ecalrobusone E (**20**),[37] guajadial C (**21**),[38] guajadial D (**22**),[38] guajadial E (**23**),[38] guajudial (**24**),[39] macrocarpal A (**25**),[40] psiguajadial H (**26**),[41] psiguajadial I (**27**),[41] psiguajadial J (**28**)[41] were isolated and identified from the leaves of guava. Among these known isolates, 14 compounds (**3**, **4**, **8**-**10**, and **12**-**20**) are reported from this plant for the first time. Although Myrtaceous plants were reported to be rich in phenol glycosides esterified with oleuropeic acid, to the best of our knowledge, this is the first report of this type of compounds from *P. guajava*.

Guava Leaf Phenolics Scavenged Free Radicals in the DPPH Assay and ROS in LPS-induced RAW264.7 Macrophages. Since guava leaf tea has been widely used

395 to treat oxidative stress related diseases,[42] antioxidative activities of these isolates were
396 evaluated with diphenylpicrylhydrazyl (DPPH) free radical scavenging assay. As
397 shown in Table 3, acylated phenolic glycosides (**1-11**) showed superior antioxidant
398 activity (IC_{50} < 200 μM except compound **3**) compared with the meroterpenoides (IC_{50}
399 > 200 μM, see Supporting Information Table S1). It was noteworthy that the antioxidant
400 activities of compounds **1**, **2**, and **5-11** (IC_{50} values ranged from 84 to 131 μM) were
401 comparable to that of positive control ascorbic acid (IC_{50} = 108.60 μM). The DPPH
402 free radical scavenging activity difference among compounds **1-11** might be due to the
403 hydroxyl group numbers, which was in agreement with previous report.[25] ROS
404 overproduction would break the balance of oxidative and antioxidative system, thereby
405 causing damage to healthy tissue cells.[2] To further confirm the antioxidant activities of
406 these acylated phenolic glycosides, ROS scavenging activity of them were evaluated in
407 RAW 264.7 macrophages. As shown in Figure 3, upon exposure to LPS for 6 h, ROS
408 levels were significantly elevated (around 2-folds) in LPS-treated negative control
409 group when compared to the non-treated control group. All of the tested compounds (**1-**
410 **11**), as well as positive control minocycline, displayed potent ROS scavenging activity
411 at 30 μM in LPS-induced RAW 264.7 cells. Moreover, compounds **5-11** exhibited
412 comparable ROS scavenging activity to the positive control minocycline (See support
413 information Table S2). The above results suggested that acylated phenolic glycosides
414 in guava leaf could reduce oxidative stress in LPS-stimulated RAW 264.7 macrophages,
415 which was in agreement with the data obtained from the DPPH free radical scavenging
416 assay. The aforementioned results highlighted the potential usage of these acylated

417 phenolic glycosides from guava leaves against oxidative stress-related chronic
418 metabolic diseases.

419 **Effects of Guava Leaf Phenolics on Nrf2 Signaling Pathway.** Nrf2 is a major
420 redox-sensitive transcription factor involved in modulating the expression of multiple
421 antioxidant target genes, and plays a crucial role in protecting macrophages from
422 damage due to elevated ROS.[24, 43] NQO1, a NAD(P)H-dependent reductase capable of
423 reducing a broad range of substrates, is an important downstream gene of Nrf2.[44]
424 Besides NQO1, GCLC is also known as a target gene of Nrf2 and plays a key role in
425 the synthesis of glutathione, as well as related cellular redox process.[45] To understand
426 the antioxidant mechanism of acylated phenolic glycosides in guava leaf, the effect of
427 compound **6** (which showed superior ROS-scavenging activity) on Nrf2 signaling
428 pathway was investigated. As showed in Figure 4, compound **6** significantly enhanced
429 the total protein levels of Nrf2, NQO1 and GCLC in LPS-stimulated RAW264.7 cells
430 at 10 and 30 μM. Our results indicated that compound **6** could act as an Nrf2 activator
431 to up-regulate the expression of its target antioxidant genes, and then reduce the
432 production of ROS in marcophages, thereby exerting antioxidant effects.

433 In summary, 28 phenolics, including 11 acylated phenolic glycosides and 17
434 meroterpenoides were isolated and identified from *P. guava* leaves. Among these
435 isolates, five are new compounds, and 14 are being reported from *P. guava* for the first
436 time. Isolated acylated phenolic glycosides display potent antioxidative activities in
437 both DPPH and ROS scavenging assay. Preliminary molecular mechanism
438 investigation reveals that acylated phenolic glycosides could active Nrf2 signaling

pathway, which reduce ROS level and exert antioxidative effects. The current study highlighted bioactive polyphenols present in guava leaf supporting its nutraceutical and functional food applications. Further *in vivo* studies are warranted to confirm the potential of these bioactive phenolics as dietary agents for the prevention and/or therapy of oxidative stress-related chronic metabolic diseases.

ASSOCIATED CONTENT

Supporting Information

IR, HRMS, and NMR spectra of compounds **1**, **2**, **5-7,** detailed information for isolation procedure and DPPH free radical scavenging activities of known compounds **12-28**, as well as cell proliferation assay result and ROS scavenging ratio of compounds **1-11** are available free of charge via the Internet at http://pubs.acs.org.

AUTHOR INFORMATION

Corresponding Authors

* Tel/Fax: 0086-24-83656122; E-mail: lyli@mail.neu.edu.cn (L.-Y. Li)

* Tel /Fax: 0086-24-83656106; E-mail: huangxs@mail.neu.edu.cn (X.-S. Huang)

Notes

The authors declare no competing financial interest.

ACKNOWLEDGMENTS

Financial support was provided by the Youth Foundation of Wuyi University (No: 2017td01), Jiangmen Program for Innovative Research Team (No: 2018630100180019806) and Foundation from Department of Education of Guangdong Province (No: 2016KCXTD005 and 2017KSYS010).

REFERENCES

(1) Umeno, A.; Biju, V.; Yoshida, Y. *In vivo* ROS production and use of oxidative stress-derived biomarkers to detect the onset of diseases such as Alzheimer's disease, Parkinson's disease, and diabetes. *Free Radic. Res.* **2017**, *51*, 413-427.

(2) Schieber, M.; Chandel, N. S. ROS function in redox signaling and oxidative stress. *Curr. Biol.* **2014**, *24*, R453-R462.

(3) NavaneethaKrishnan, S.; Rosales, J. L.; Lee, K. Y. ROS-mediated cancer cell killing through dietary phytochemicals. *Oxid. Med. Cell Longev.* **2019**, *2019*, 9051542.

(4) Koch, W. Dietary polyphenols-important non-nutrients in the prevention of chronic noncommunicable diseases. A systematic review. *Nutrients* **2019**, *11*, pii: E1039.

(5) Akhtar, M. J.; Ahamed, M.; Alhadlaq, H. A.; Alshamsan, A. Mechanism of ROS scavenging and antioxidant signalling by redox metallic and fullerene nanomaterials: Potential implications in ROS associated degenerative disorders. *Biochim. Biophys. Acta Gen. Subj.* **2017**, *1861*, 802-813.

(6) Ullah, R.; Khan, M.; Shah, S. A.; Saeed, K.; Kim, M. O. Natural antioxidant anthocyanins-A hidden therapeutic candidate in metabolic disorders with major focus in neurodegeneration. *Nutrients* **2019**, *11*, pii: E1195.

(7) Ci, X.; Zhou, J.; Lv, H.; Yu, Q.; Peng, L.; Hua, S. Betulin exhibits anti-inflammatory activity in LPS-stimulated macrophages and endotoxin-shocked mice through an AMPK/AKT/Nrf2-dependent mechanism. *Cell Death Dis.* **2017**, *8*, e2798.

(8) Ci, X.; Lv, H.; Wang, L.; Wang, X.; Peng, L.; Qin, F. X.-F.; Cheng, G. The antioxidative potential of farrerol occurs via the activation of Nrf2 mediated HO-1 signaling in RAW 264.7 cells. *Chem. Biol. Interact.* **2015**, *239*, 192-199.

(9) Zhou, Y.; Jiang, Z.; Jia, G.; Shi, J. Recent advances of natural polyphenols activators for Keap1-Nrf2 signaling pathway. *Chem. Biodivers.* **2019**, DOI: 10.1002/cbdv.201900400.

(10) Stefanson, L. A.; Bakovic, M. Dietary regulation of Keap1/Nrf2/ARE pathway: focus on plant-derived compounds and trace minerals. *Nutrients* **2014**, *6*, 3777-3801.

(11) Zhu, X.; Ouyang, W.; Pan, C.; Gao, Z.; Han, Y.; Song, M.; Feng, K.; Xiao, H.;

490 Cao, Y. Identification of a new benzophenone from *Psidium guajava* L. leaves and its
491 antineoplastic effects on human colon cancer cells. *Food Funct.* **2019**, *10*, 4189-4198.
492 (12) Qin, X.; Yu, Q.; Yan, H.; Khan, A.; Feng, M.; Li, P.; Hao, X.; An, L.; Liu, H.
493 Meroterpenoids with antitumor activities from Guava (*Psidium guajava*). *J. Agric.*
494 *Food Chem.* **2017**, *65*, 4993-4999.
495 (13) Wang, L.; Liu, Y.; Luo, Y.; Huang, K.; Wu, Z. Quickly screening for potential
496 alpha-glucosidase inhibitors from guava leaves tea by bioaffinity ultrafiltration coupled
497 with HPLC-ESI-TOF/MS method. *J. Agric. Food Chem.* **2018**, *66*, 1576-1582.
498 (14) Chang, C.; Hsieh, C. L.; Wang, H.; Peng, C.; Chyau, C. C.; Peng, R. Y. Unique
499 bioactive polyphenolic profile of guava (*Psidium guajava*) budding leaf tea is related
500 to plant biochemistry of budding leaves in early dawn. *J. Sci. Food Agric.* **2013**, *93*,
501 944-954.
502 (15) Wang, L.; Wu, Y.; Bei, Q.; Shi, K.; Wu, Z. Fingerprint profiles of flavonoid
503 compounds from different *Psidium guajava* leaves and their antioxidant activities. *J.*
504 *Sep. Sci.* **2017**, *40*, 3817-3829.
505 (16) Diaz-de-Cerio, E.; Pasini, F.; Verardo, V.; Fernandez-Gutierrez, A.; Segura-
506 Carretero, A.; Caboni, M. F. *Psidium guajava* L. leaves as source of proanthocyanidins:
507 Optimization of the extraction method by RSM and study of the degree of
508 polymerization by NP-HPLC-FLD-ESI-MS. *J. Pharm. Biomed. Anal.* **2017**, *133*, 1-7.
509 (17) Li, C.; Ma, J.; Sun, H.; Zhang, D.; Zhang, D. Guajavadimer A, a dimeric
510 caryophyllene-derived meroterpenoid with a new carbon skeleton from the leaves of
511 *Psidium guajava*. *Org. Lett.* **2016**, *18*, 168-171.
512 (18) Heskes, A. M.; Goodger, J. Q.; Tsegay, S.; Quach, T.; Williams, S. J.; Woodrow,
513 I. E. Localization of oleuropeyl glucose esters and a flavanone to secretory cavities of
514 Myrtaceae. *PLoS One* **2012**, *7*, e40856.
515 (19) Tian, L.; Zhang, Y.; Wang, Y.; Lai, C.; Yang, C. Eucalmaidins A−E, (+)-
516 oleuropeic acid derivatives from the fresh leaves of *Eucalyptus maideni*. *J. Nat. Prod.*
517 **2009**, *72*, 1608-1611.
518 (20) Tian, L.; Zhang, Y.; Qu, C.; Wang, Y.; Yang, C. Phloroglucinol glycosides from
519 the fresh fruits of *Eucalyptus maideni*. *J. Nat. Prod.* **2010**, *73*, 160-163.

(21) Ito, H.; Koreishi, M.; Tokuda, H.; Nishino, H.; Yoshida, T. Cypellocarpins A−C, phenol glycosides esterified with oleuropeic acid, from *Eucalyptus cypellocarpa*. *J. Nat. Prod.* **2000**, *63,* 1253-1257.

(22) Hasegawa, T.; Takano, F.; Takata, T.; Niiyama, M.; Ohta, T. Bioactive monoterpene glycosides conjugated with gallic acid from the leaves of *Eucalyptus globulus*. *Phytochemistry* **2008,** *69*, 747-753.

(23) Hou, A.; Liu, Y.; Yang, H.; Lin, Z.; Sun, H. Hydrolyzable tannins and related polyphenols from *Eucalyptus globulus*. *J. Asian Nat. Prod. Res.* **2000,** *2*, 205-212.

(24) Li, T.; Cheng, X.; Du, M.; Chen, B.; Mao, X. Upregulation of heme oxygenase-1 mediates the anti-inflammatory activity of casein glycomacropeptide (GMP) hydrolysates in LPS-stimulated macrophages. *Food Funct.* **2017**, *8*, 2475-2484.

(25) Liu, F.; Ma, H.; Wang, G.; Liu, W.; Seeram, N. P.; Mu, Y.; Xu, Y.; Huang, X.; Li, L. Phenolics from *Eugenia jambolana* seeds with advanced glycation endproduct formation and alpha-glucosidase inhibitory activities. *Food Funct.* **2018**, *9*, 4246-4254.

(26) Han, L.; Gao, C.; Jiang, Y.; Guan, P.; Liu, J.; Li, L.; Xu, L.; Huang, X. Jiangrines A-F and jiangolide from an actinobacterium, *Jiangella gansuensis*. *J. Nat. Prod.* **2014**, *77*, 2605-2610.

(27) Zhang, Y.; Chen, Y. Isobiflorin, a chromone *C*-glucoside from cloves (*Eugenia Caryophyllata*). *Phytochemistry* **1997**, *45*, 401-403.

(28) Ito, H.; Kasajima, N.; Tokuda, H.; Nishino, H.; Yoshida, T. Dimeric flavonol glycoside and galloylated *C*-glucosylchromones from *Kunzea ambigua*. *J. Nat. Prod.* **2004**, *67*, 411-415.

(29) Kasajima, N.; Ito, H.; Hatano, T.; Yoshida, T.; Kaneda, M. Cypellogins A, B and C, acylated flavonol glycosides from *Eucalyptus cypellocarpa*. *Chem. Pharm. Bull.* **2005**, *53*, 1345-1347.

(30) Yoshida, K.; Hishida, A.; Iida, O.; Hosokawa, K.; Kawabata, J. Flavonol caffeoylglycosides as alpha-glucosidase inhibitors from *Spiraea cantoniensis* flower. *J. Agric. Food Chem.* **2008**, *56*, 4367-4371.

(31) Begum, S.; Farhat; Siddiqui, B. S. Chromenone glucosides acylated with monoterpene acids from the leaves of *Eucalyptus camaldulensis var. obtusa*. *Helv.*

Chim. Acta **2011**, *94*, 238-247.

(32) Wu, H.; Li, X.; Li, R.; Li, L.; Wang, N. Study on anti-oxidative components from leaves of *Psidium guajava*. *Chin. Trad. Herb. Drugs* **2010**, *41*, 1593-1597.

(33) Takasaki, M.; Konoshima, T.; Kozuka, M.; Haruna, M.; Ito, K.; Yoshida, S. Four euglobals from *Eucalyptus blakelyi*. *Chem. Pharm. Bull.* **1994**, *42*, 2177-2179.

(34) Kozuka, M.; Sawada, T.; Kasahara, F.; Mizuta, E.; Amano, T.; Komiya, T.; Goto, M. The granulation-inhibiting principles from *Eucalyptus globulus* Labill. II. The structures of euglobal-Ia_1, euglobal-Ia_2, euglobal-Ib, euglobal-Ic, euglobal-IIa, euglobal-IIb, and euglobal-IIc. *Chem. Pharm. Bull*. **1982**, *30*, 1952-1963.

(35) Kozuka, M.; Sawada, T.; Mizuta, E.; Kasahara, F.; Amano, T.; Komiya, T.; Goto, M. The granulation-inhibiting principles from *Eucalyptus globulus* Labill. III. The structures of euglobal-III, -IVb and -VII. *Chem. Pharm. Bull.* **1982**, *30*, 1964-1973.

(36) Takasaki, M.; Konoshima, T.; Kozuka, M.; Haruna, M.; Ito, K.; Crow, W. D.; *Pat*on, D. M. Euglobal-In-1, a new euglobal from *Eucalyptus incrassata. Chem. Pharm. Bull.* **1994**, *42,* 2113-2116.

Four euglobals from *Eucalyptus blakelyi*. *Chem. Pharm. Bull.* **1994,** *42*, 2177-2179.

(37) Liu, H.; Feng, M.; Yu, Q.; Yan, H.; Zeng, Y.; Qin, X.; He, L.; Liu, H. Formyl phloroglucinol meroterpenoids from *Eucalyptus tereticornis* and their bioactivities. *Tetrahedron* **2018**, *74*, 1540-1545.

(38) Gao, Y.; Li, G.; Li, Y.; Hai, P.; Wang, F.; Liu, J. Guajadials C-F, four unusual meroterpenoids from *Psidium guajava*. *Nat. Prod. Bioprosp.* **2013**, *3*, 14-19.

(39) Yang, X.; Hsieh, K.; Liu, J. Guajadial: an unusual meroterpenoid from guava leaves *Psidium guajava*. *Org. Lett.* **2007**, *9*, 5135-5138.

(40) Nishizawa, M.; Emura, M.; Kan, Y.; Yamada, H.; Ogawa, K.; Hamanaka, N. Macrocarpals: HIV-RTase inhibitors of *Eucalyptus globulus*. *Tetrahedron Lett.* **1992**, *33*, 2983-2986.

(41) Tang, G.; Dong, Z.; Guo, Y.; Cheng, Z.; Zhou, C.; Yin, S. Psiguajadials A–K: Unusual psidium meroterpenoids as phosphodiesterase-4 inhibitors from the leaves of *Psidium guajava*. *Sci. Rep.* **2017**, *7*, 1047.

(42) Luo, Y.; Peng, B.; Wei, W.; Tian, X.; Wu, Z. Antioxidant and anti-diabetic

580 activities of polysaccharides from guava leaves. *Molecules* **2019**, *24*, pii: E1343.
581 (43) Luo, J.; Shen, X.; Lio, C. K.; Dai, Y.; Cheng, C.; Liu, J.; Yao, Y.; Yu, Y.; Xie, Y.;
582 Luo, P.; Yao, X.; Liu, Z.; Zhou, H. Activation of Nrf2/HO-1 pathway by nardochinoid
583 C inhibits inflammation and oxidative stress in lipopolysaccharide-stimulated
584 macrophages. *Front Pharmacol.* **2018**, *9*, 911.
585 (44) Liu, C.; Cui, Y.; Pi, F.; Guo, Y.; Cheng, Y.; Qian, H. Torularhodin ameliorates
586 oxidative activity *in vitro* and D-galactose-induced liver injury via the Nrf2/HO-1
587 signaling pathway *in vivo*. *J. Agric. Food Chem.* **2019**, DOI: 10.1021/acs.jafc.9b03847.
588 (45) Sikalidis, A. K.; Mazor, K. M.; Lee, J. I.; Roman, H. B.; Hirschberger, L. L.;
589 Stipanuk, M. H. Upregulation of capacity for glutathione synthesis in response to amino
590 acid deprivation: regulation of glutamate-cysteine ligase subunits. *Amino Acids* **2014**,
591 *46*, 1285-1296.

FIGURE CAPTIONS

Figure 1. Structures of compounds **1-11**.

Figure 2. Key ^{1}H-^{1}H COSY and HMBC correlations of compounds **2** and **5**

Figure 3. Effect of compounds **1-11** on the production of ROS in LPS-stimulated RAW 264.7 macrophages. Data are the mean ± SD for three independent experiments. ### $p < 0.001$ vs. control group; ** $p < 0.01$, *** $p < 0.001$ vs. LPS group.

Figure 4. Effects of compound **6** on the protein expression of Nrf2, GCLC and NQO1 in LPS-stimulated RAW 264.7 macrophages. RAW 264.7 cells were pretreated with different concentrations of compound **6** (3.3, 10 or 30 μM) for 2 h, followed by exposure to LPS (1 μg/mL) for additional 6 h. The cells were lysed with RIPA buffer and the protein levels for total Nrf2, GCLC and NQO1were measured by using immunoblot analysis. β-actin was used as a loading control. MINO was used as positive control. And all the experiments have been repeated three times independently. Data presented as mean ± S.E., n = 3. # $p < 0.05$, ## $p < 0.01$ as compared with the control group; * $p < 0.05$, ** $p < 0.01$, *** $p < 0.001$ as compared with the LPS group.

Table 1. ^{1}H (600 MHz) and ^{13}C NMR (150 MHz) Data for Compounds **1**, **2** and **5**

	1		**2**		**5**	
Position	^{13}C, type	^{1}H (*J* in Hz)	^{13}C, type	^{1}H (*J* in Hz)	^{13}C, type	^{1}H (*J* in Hz)
Aglycon						
1					136.9 C	
2	167.1, C		170.0, C		105.3 CH	7.04 s
3	107.9, CH	6.14 s	108.5, CH	6.17 s	152.9 C	
4	182.2, C		182.4, C		136.9 C	
5	160.9, C		161.1, C		150.4 C	
6	99.4, CH	6.18 s	98.2, CH	6.16 s	111.1 CH	7.08 s
7	165.1, C		163.0, C		168.4 C	
8	104.6, C		103.1, C			
9	157.1, C		157.4, C			
10	103.4, C		104.1, C			
2-isobutyl						
			43.0, CH_2	2.52 d (7.2)		
			26.9, CH	2.26 m		
			22.7, CH_3	1.00 d (6.6)		
			22.7, CH_3	1.00 d (6.6)		
2-CH_3	20.1, CH_3	2.31 s				
3-OCH_3					56.5 CH_3	3.72 s
5-OH		13.00 s		12.99 s		
Sugar residue						
1′	74.1, CH	4.64 d (10.2)	70.9, CH	4.82 d (10.2)	104.3 CH	4.78 d (7.2)
2′	71.3, CH	3.93 t (9.6)	72.6, CH	5.42 t (10.2)	74.4 CH	3.32 m
3′	78.9, CH	3.24 m	76.2, CH	3.47 m	76.5 CH	3.26 m
4′	70.6, CH	3.30 m	71.4, CH	3.20 m	70.7 CH	3.19 m
5′	78.5, CH	3.42 m	82.2, CH	3.25 m	74.6 CH	3.39 m
6′	64.3, CH_2	4.10 m	62.1, CH_2	3.47 m	63.9 CH_2	4.02 m
		4.30 m		3.75 m		4.35 dd (11.4; 1.8)
Monoterpene residue						
1″	130.1, C		129.9, C		129.9 C	
2″	140.4, CH	6.90 m	139.8, CH	6.69 m	140.6 CH	6.81 s
3″	27.5, CH_2	1.94 m	27.3, CH_2	1.84 m	27.5 CH_2	1.91 m
		2.23 m		2.14 m		2.22 m
4″	44.2, CH	1.39 m	44.1, CH	1.28 m	44.2 CH	1.37 m
5″	23.4, CH_2	1.07 m	23.3, CH_2	1.30 m	23.4 CH_2	1.06 m
		1.90 m		1.81 m		1.89 m
6″	25.4, CH_2	2.01 m	25.4, CH_2	1.85 m	25.3 CH_2	1.96 m
		2.37 m		2.13 m		2.31 m
7″	166.8, C		166.1, C		166.6 C	
8″	70.6, C		70.6, C		70.7 C	
9″	27.0, CH_3	1.05 s	26.9, CH_3	1.01 s	26.9 CH_3	1.06 s
10″	27.5, CH_3	1.05 s	27.5, CH_3	1.01 s	27.6 CH_3	1.06 s

Table 2. ^{1}H (600 MHz) and ^{13}C NMR (150 MHz) Data for Compounds **6** and **7**

	6		**7**	
Position	^{13}C, type	^{1}H (*J* in Hz)	^{13}C, type	^{1}H (*J* in Hz)
Aglycon				
2	156.7, C		157.0, C	
3	133.2, C		133.3, C	
4	177.8, C		177.3, C	
5	161.7, C		161.5, C	
6	99.2, CH	6.17 s	99.9, CH	6.09 s
7	164.8, C		166.4, C	
8	93.9, CH	6.38 s	94.3, CH	6.31 s
9	156.8, C		157.0, C	
10	104.2, C		103.1, C	
1′	121.5, C		121.0, C	
2′	115.6, CH	7.50 s	115.6, CH	7.48 d (1.8)
3′	145.3, C		145.5, C	
4′	148.9, C		148.8, C	
5′	116.5, CH	6.82 d (8.4)	115.9, CH	6.80 d (8.4)
6′	121.9, CH	7.52 d (8.4)	122.4, CH	7.63 dd (8.4; 1.8)
5-OH		12.65 s		12.63 s
Sugar residue				
1″	100.7, CH	5.53 d (7.2)	101.9, CH	5.45 d (8.4)
2″	74.3, CH	3.28 m	73.5, CH	3.64 m
3″	76.8, CH	3.26 m	71.4, CH	3.58 m
4″	70.7, CH	3.15 m	68.9, CH	3.62 m
5″	74.7, CH	3.33 m	73.5, CH	3.41 m
6″	63.5, CH_2	3.95 m	63.9, CH_2	4.05 m
		4.25 d (11.4)		
Monoterpene residue				
1‴	129.6, C		129.6, C	
2‴	139.3, CH	6.60 m	139.3, CH	6.59 br s
3‴	30.7, CH_2	1.81 m	30.6, CH_2	1.79 m
		2.09 m		2.07 m
4‴	39.5, CH	1.92 m	39.1, CH	1.90 m
5‴	26.8, CH_2	1.16 m	26.8, CH_2	1.15 m
		1.62 m		1.60 m
6‴	24.4, CH_2	1.85 m	24.4, CH_2	1.84 m
		2.09 m		2.07 m
7‴	166.3, C		166.4, C	
8‴	149.0, C		148.8, C	
9‴	109.7, CH_2	4.67 s	109.7, CH_2	4.65 s
		4.72 s		4.71 s
10‴	21.1, CH_3	1.69 s	21.0, CH_3	1.68 s

Table 3. DPPH free radical scavenging activity of compounds **1−11**

No.	IC_{50} (μM)
1	131.87 ± 4.12
2	113.33 ± 3.44
3	> 200
4	180.00 ± 3.57
5	114.94 ± 3.19
6	97.68 ± 1.88
7	97.05 ± 7.83
8	103.95 ± 0.06
9	98.75 ± 1.22
10	92.55 ± 4.03
11	84.28 ± 4.68
Ascorbic acid[a]	108.60 ± 5.63

[a]Positive control substance

Figure 1.

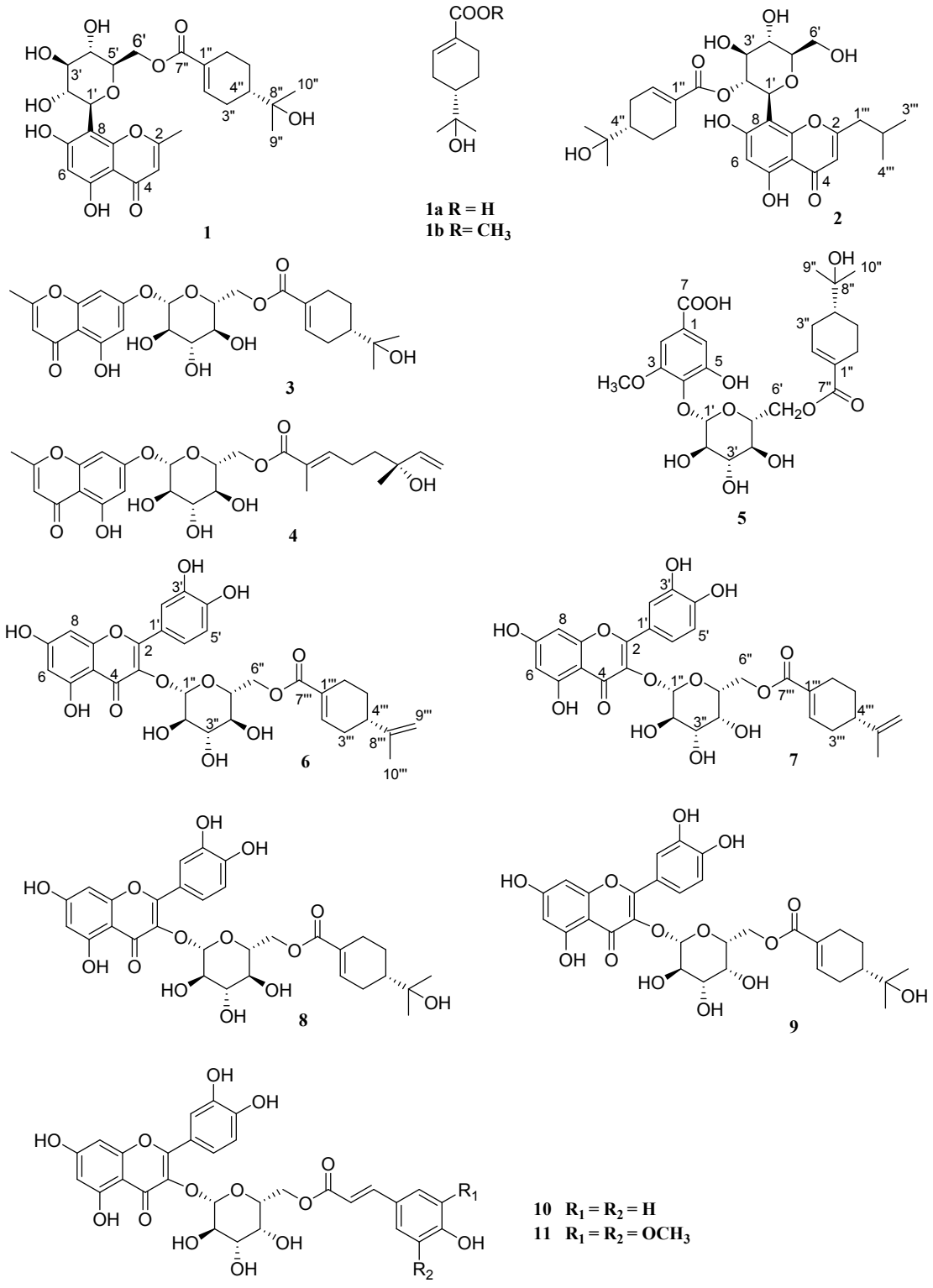

Figure 2.

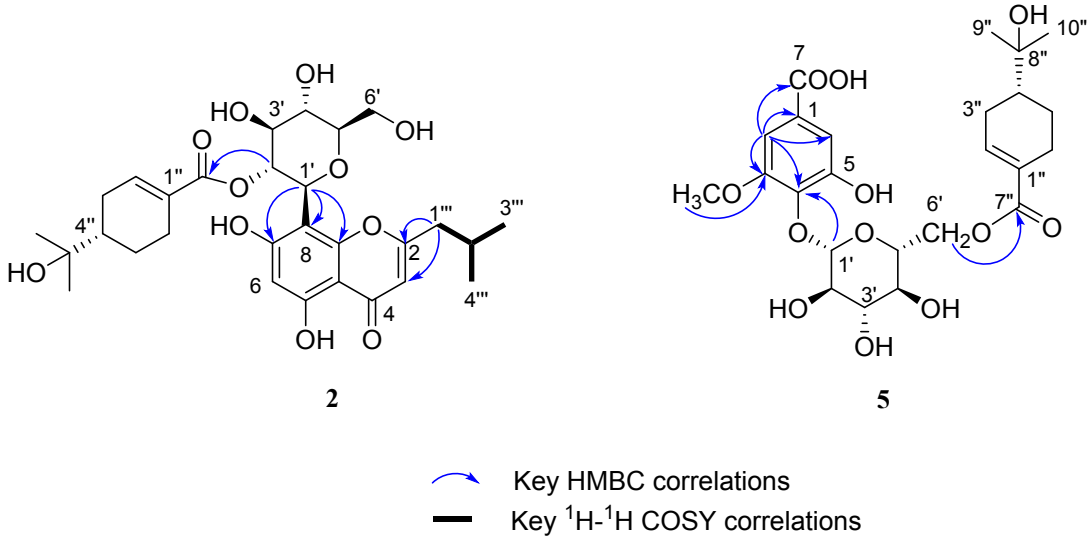
OH
HO
3'
6'
OH
O
1"
1'
O
O
HO
1'''
3'''
4"
8
2
HO
6
4'''
4
OH
O
2
7
COOH
1
9"
OH
10"
8"
3"
1"
5
H3CO
OH
6'
7"
O
CH2O
O
O
1'
3'
HO
OH
OH
Key HMBC correlations
Key 1H-1H COSY correlations

2 **5**

Figure 3.

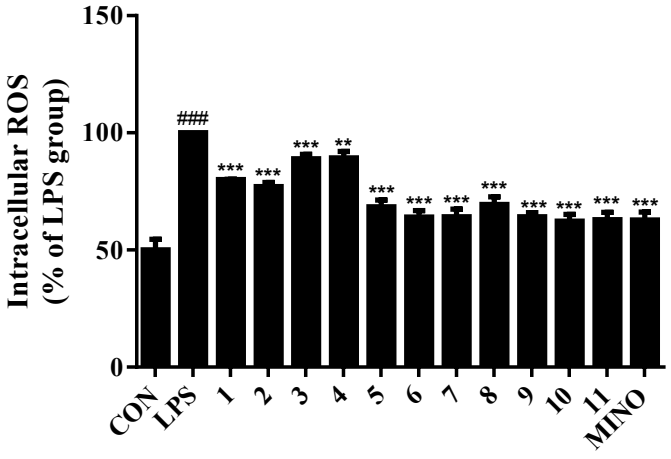
Intracellular ROS
(% of LPS group)
150
100
50
0
###
***
***
***
**
***
***
***
***
***
***
***
***
CON
LPS
1
2
3
4
5
6
7
8
9
10
11
MINO

Figure 4.

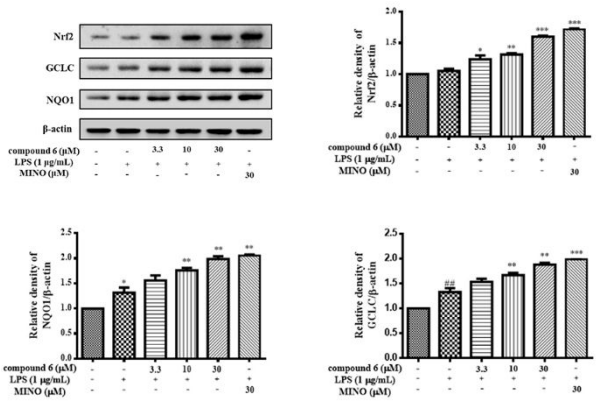
Nrf2
GCLC
NQO1
β-actin
compound 6 (μM) - - 3.3 10 30 -
LPS (1 μg/mL) - + + + + +
MINO (μM) - - - - - 30
Relative density of Nrf2/β-actin
Relative density of NQO1/β-actin
Relative density of GCLC/β-actin

Table of Contents Graphic